

## RESEARCH ARTICLE

## A novel substrate for arrhythmias in Chagas disease

Artur Santos-Miranda<sup>1</sup>, Julliane V. Joviano-Santos<sup>1</sup>, Jaqueline O. Sarmiento<sup>1</sup>, Alexandre D. Costa<sup>2</sup>, Allysson T. C. Soares<sup>3</sup>, Fabiana S. Machado<sup>3</sup>, Jader S. Cruz<sup>1,2,3\*</sup>, Danilo Roman-Campos<sup>1\*</sup>

**1** Department of Biophysics, Universidade Federal de São Paulo, São Paulo, Brazil, **2** Department of Pharmacology and Physiology, Biological Sciences Institute, Universidade Federal de Minas Gerais, Minas Gerais, Brazil, **3** Department of Biochemistry and Immunology, Biological Sciences Institute, Universidade Federal de Minas Gerais, Minas Gerais, Brazil

\* [jcruz@icb.ufmg.br](mailto:jcruz@icb.ufmg.br) (JSC); [drcampos@unifesp.br](mailto:drcampos@unifesp.br) (DRC)



## Abstract

## Background

Chagas disease (CD) is a neglected disease that induces heart failure and arrhythmias in approximately 30% of patients during the chronic phase of the disease. Despite major efforts to understand the cellular pathophysiology of CD there are still relevant open questions to be addressed. In the present investigation we aimed to evaluate the contribution of the Na<sup>+</sup>/Ca<sup>2+</sup> exchanger (NCX) in the electrical remodeling of isolated cardiomyocytes from an experimental murine model of chronic CD.

## Methodology/Principal findings

Male C57BL/6 mice were infected with Colombian strain of *Trypanosoma cruzi*. Experiments were conducted in isolated left ventricular cardiomyocytes from mice 180–200 days post-infection and with age-matched controls. Whole-cell patch-clamp technique was used to measure cellular excitability and Real-time PCR for parasite detection. In current-clamp experiments, we found that action potential (AP) repolarization was prolonged in cardiomyocytes from chagasic mice paced at 0.2 and 1 Hz. After-depolarizations, both subthreshold and with spontaneous APs events, were more evident in the chronic phase of experimental CD. In voltage-clamp experiments, pause-induced spontaneous activity with the presence of diastolic transient inward current was enhanced in chagasic cardiomyocytes. AP waveform disturbances and diastolic transient inward current were largely attenuated in chagasic cardiomyocytes exposed to Ni<sup>2+</sup> or SEA0400.

## Conclusions/Significance

The present study is the first to describe NCX as a cellular arrhythmogenic substrate in chagasic cardiomyocytes. Our data suggest that NCX could be relevant to further understanding of arrhythmogenesis in the chronic phase of experimental CD and blocking NCX may be a new therapeutic strategy to treat arrhythmias in this condition.

## OPEN ACCESS

**Citation:** Santos-Miranda A, Joviano-Santos JV, Sarmiento JO, Costa AD, Soares ATC, Machado FS, et al. (2021) A novel substrate for arrhythmias in Chagas disease. *PLoS Negl Trop Dis* 15(6): e0009421. <https://doi.org/10.1371/journal.pntd.0009421>

**Editor:** Juan M. Bustamante, University of Georgia, UNITED STATES

**Received:** October 16, 2020

**Accepted:** April 28, 2021

**Published:** June 2, 2021

**Copyright:** © 2021 Santos-Miranda et al. This is an open access article distributed under the terms of the [Creative Commons Attribution License](https://creativecommons.org/licenses/by/4.0/), which permits unrestricted use, distribution, and reproduction in any medium, provided the original author and source are credited.

**Data Availability Statement:** All relevant data are within the manuscript and its [Supporting Information](#) files.

**Funding:** DRC received funding from the Fundação de Amparo à Pesquisa do Estado de São Paulo (<https://fapesp.br/>) (grant no. 2014/09861-1 and grant no. 2019/21304-4). ASM received a postdoctoral fellowship from the Fundação de Amparo à Pesquisa do Estado de São Paulo (<https://fapesp.br/bolsas/pd>) (grant no. 2018/22830-9). JVJS received a postdoctoral fellowship

from the Fundação de Amparo à Pesquisa do Estado de São Paulo (<https://fapesp.br/bolsas/pd>) (grant no. 2018/20777-3). JOS received a master student fellowship from the Fundação de Amparo à Pesquisa do Estado de São Paulo (<https://fapesp.br/bolsas/ms>) (grant no. 2020/09403-4). JSC received funding from Conselho Nacional de Desenvolvimento Científico e Tecnológico (<https://www.gov.br/cnpq/pt-br>) (grant no. 312474/2017-2 and grant no. 437969/2018-5). DRC received funding from Conselho Nacional de Desenvolvimento Científico e Tecnológico (<https://www.gov.br/cnpq/pt-br>) (grant no. 304257/2020-6). FSM received a grant from National Institute for Science and Technology in Dengue and Host-microbial interactions (<http://labs.icb.ufmg.br/inctemdengue/>) (grant no. APQ-03606-17). FSM received a grant from Fundação de Amparo à Pesquisa do Estado de Minas Gerais, Rede Mineira de Imunobiológicos (<https://fapemig.br/pt/>) (grant no. 00140-16). The funders had no role in study design, data collection and analysis, decision to publish, or preparation of the manuscript.

**Competing interests:** The authors have declared that no competing interests exist.

## Author summary

Chagas disease (CD), caused by the parasite *Trypanosoma cruzi*, is a neglected disease that induces heart failure and arrhythmias in approximately 30% of patients during the chronic phase of the disease. There are several substrates for arrhythmias in the heart. Some of them involve changes in the electrical properties of cardiomyocytes, the working cells of the heart. In our study we evaluate the potential involvement of Na<sup>+</sup>/Ca<sup>2+</sup> exchanger (NCX) in the arrhythmic phenotype of cardiomyocytes isolated from mice infected with *Trypanosoma cruzi*, between 180- and 200- days post-infection, which is considered the chronic phase of CD in this animal model. In our study we found several arrhythmogenic membrane potential oscillations during action potential measurements, in rest and using a protocol to simulate a pause after a tachycardia. Using pharmacological approach, we determine that NCX significantly contributed to the arrhythmogenic phenomena observed. Thus, in our study we demonstrate that NCX may be relevant to the cellular arrhythmogenic profile observed in cardiomyocytes during the chronic phase of experimental CD and blocking NCX may be a new therapeutic strategy to treat arrhythmias in this condition.

## Introduction

Chagas disease (CD) is a vector-borne disease caused by the parasite *Trypanosoma cruzi* that affects 6 to 7 million people worldwide, mostly in Latin America. Although the original route of transmission occurs through the triatomine vector, additional routes, including contaminated food and vertical transmission further contributes to increase the spread of the disease [1]. In 2016 it was estimated that in the United States there were approximately 238.000 reported cases of CD [2], but the number may be higher [3]. Around 30% of all infected individuals experience severe cardiac complications during the chronic phase of the disease leading to Chagasic CardioMyopathy (CCM). Clinical manifestations include non-sustained and sustained ventricular tachycardia and heart failure that, if not properly dealt with, will culminate in death [4]. Despite the severity of CCM, it is rather difficult to indicate proper therapeutic agents due to the incomplete knowledge of cellular biophysical mechanisms responsible for the generation of cardiac arrhythmias.

In experimental models of CD it was found that cardiomyocytes from infected mice displayed severe electromechanical remodeling [5–8]. Major changes were observed in action potential (AP) repolarization and a consistent reduction of L-type Ca<sup>2+</sup> current density [6,7,9,10]. However, there are still important and relevant questions to be addressed in the context of the molecular pathophysiology of CCM. Thus, in the present study, an experimental murine model of chronic CCM was used to directly access the possible contribution of Na<sup>+</sup>/Ca<sup>2+</sup> exchange current (I<sub>NCX</sub>) in the electrical remodeling of cardiomyocytes during chronic experimental CD [5,7].

## Methods

### Ethics statement

All animal related procedures were previously approved by the Institutional Animal Care and Use Committee (protocol #1948230414). All animal experiments were in accordance with the [ARRIVE guidelines](#) and were carried out in accordance with the U.K. Animals (Scientific

Procedures) Act, 1986 and associated guidelines, [EU Directive 2010/63/EU for animal experiments](#).

### Animals

We used male C57BL/6 mice 8 weeks-old obtained from CEBIO (ICB, UFMG, Belo Horizonte, MG, Brazil). Control and experimental groups were studied between 180- and 200- days after saline injection or post infection (d.p.i.).

### Infection

The Colombian strain of *T. cruzi* (DTU TcI) [11] was used in all experiments. Trypomastigotes were maintained by blood passage in Swiss mice every 7 days. Trypomastigotes were obtained from heparinized blood, counted, and used for infection. Mice were injected in the peritoneal cavity with 100 trypomastigotes, as previously described. Control mice received the same treatment, except by the absence of *T. cruzi*. [6,7,10,12].

### Cardiomyocyte isolation

Freshly isolated left ventricular cardiomyocytes (LVC) were obtained following a previously described method [13]. After isolation, cardiomyocytes were kept in Tyrode's solution at room temperature (25°C). Experiments were conducted up to 4 h after LVC isolation. Usually 60–80% of viable LVC was obtained after cell isolation.

### Cellular electrophysiology

Whole-cell patch-clamp recordings were obtained using an EPC-10 patch-clamp amplifier (HEKA, Holliston, Massachusetts, USA) in the voltage- and current-clamp modes [6]. Glass pipettes were pulled with 0.5–1.5 M $\Omega$  tip resistance and cells with series resistance higher than 8 M $\Omega$  were not considered in the analysis. To achieve better voltage control, all ion current measurements were electronically compensated for series resistance (60–70%). In all records, cells were bathed with regular Tyrode's solution. After break-in, cells were kept resting for 2–3 minutes, in order to allow proper equilibration. For internal and external solutions see [S1 Table](#).

### Action potential and pause-induced transient current recordings

Action potentials (AP) were triggered using a rectangular (5–7 ms duration) depolarizing current pulses (1 nA). Electrical stimulation frequencies were set at 0.2 and 1 Hz. AP recordings were sampled at 10 kHz. Using Clampfit (Molecular Devices, v10.5) we analyzed time to 50 and 90% of AP repolarization (APR<sub>50</sub> and APR<sub>90</sub>, respectively), maximal rate of AP depolarization (V/s), overshoot (mV) and resting membrane potential (mV). Stimulation protocols designed to mimic mouse ventricular AP were used to explore whether membrane currents underlying spontaneous activity could be detected under the same experimental conditions used during conventional current-clamp experiments.

Transient inward current ( $I_{Ti}$ ) area was calculated by defining a baseline diastolic current and measuring the area of 9 s of diastolic recording after application of the tachycardia protocol. For some experiments, AP and  $I_{Ti}$  were recorded prior and after superfusion of extracellular solution containing Ni<sup>+</sup> or SEA0400. Details are given in figure legends.

### **Na<sup>+</sup>/Ca<sup>2+</sup> exchange current recordings, and Sarcoplasmic reticulum Ca<sup>2+</sup> content**

Sarcoplasmic reticulum (SR) Ca<sup>2+</sup> content was measured in cardiomyocytes held at -80 mV and the membrane potential was depolarized to 0 mV (100 ms) and clamped back to -80 mV. This protocol was repeated every other second for 30 s to achieve steady-state conditions. SR Ca<sup>2+</sup> content was then estimated by rapidly switching to a solution containing 10 mM of caffeine to cause SR Ca<sup>2+</sup> release. In the continued presence of caffeine, the SR is unable to reaccumulate Ca<sup>2+</sup> and extrusion of Ca<sup>2+</sup> is mainly due to I<sub>NCX</sub>. To directly measure I<sub>NCX</sub> a ramp protocol (0.012 V/s) from +40 to -70 mV every 10 s was applied. Holding membrane potential was set at -30 mV.

### **Real-time PCR for parasite detection in isolated left ventricular cardiomyocytes**

Isolated LVC were removed and total RNA was isolated and estimated by real time PCR (polymerase chain reaction). RNA was extracted using TRIzol (Thermo Fisher) and reverse transcription was performed using 500ng of total RNA with iScript Reverse Transcriptase (Biorad) and iScript Reaction Mix (Biorad) in a final reaction volume of 10 µl. Real-time quantitative PCR (qPCR) was performed on an CFX96 real time system (Biorad, Laboratories) using SYBR green PCR master mix (Applied Biosystems) with primers for *T. cruzi* 18S (18S forward TTGTTTGGTTGATTCCGTCA; 18S reverse CCCAGAACATTGAGGAGCAT) and 18S endogenous (mouse) were (18S forward: CTC AACACGGGAAACCTCA; 18S reverse: CGTTCACC AACTAAGAACG). The threshold cycle (Ct) and the normalized relative expression levels for the *T. cruzi* 18S to mice endogenous 18S (LVC) were determined by the ΔCt method.

### **Statistical analysis**

Data are presented as means ± standard error of mean (SE), unless when indicated. Statistical significance was determined by paired sample t-test, two-sample t-test, one-way and two-way ANOVA (followed by Tukey's post-hoc test), after verification of normality using Kolmogorov-Smirnov test. The frequency of "aberrant" AP waveforms and I<sub>T1</sub> were tested with Fisher's exact test. The statistical test is indicated in figure legend. Significance was set at p < 0.05. Data were analyzed using Excel (Microsoft Co. USA) and Origin 8.0 (OriginLab Co. USA).

## **Results**

### **Prolongation of action potential duration is frequency-dependent in experimental Chagas disease**

Previous studies on experimental CD have found prolongation of cardiomyocyte AP repolarization [6,7,9,10]. However, in most of these studies sarcoplasmic Ca<sup>2+</sup> was strongly chelated which probably had attenuated the participation of membrane Ca<sup>2+</sup>-dependent conductance. Thus, we decided to revisit the AP waveform in isolated LVC in the chronic phase of experimental CD. Fig 1A shows representative traces of AP recorded at 0.2 and 1 Hz. Fig 1B represents time to 50 and 90% of AP repolarization (APR). At 0.2 and 1 Hz a substantial increase in 90% of APR was observed when comparing healthy and diseased LVC, in agreement with previous results [7,10]. In addition, resting membrane potential was affected by CCM (S2 Table).

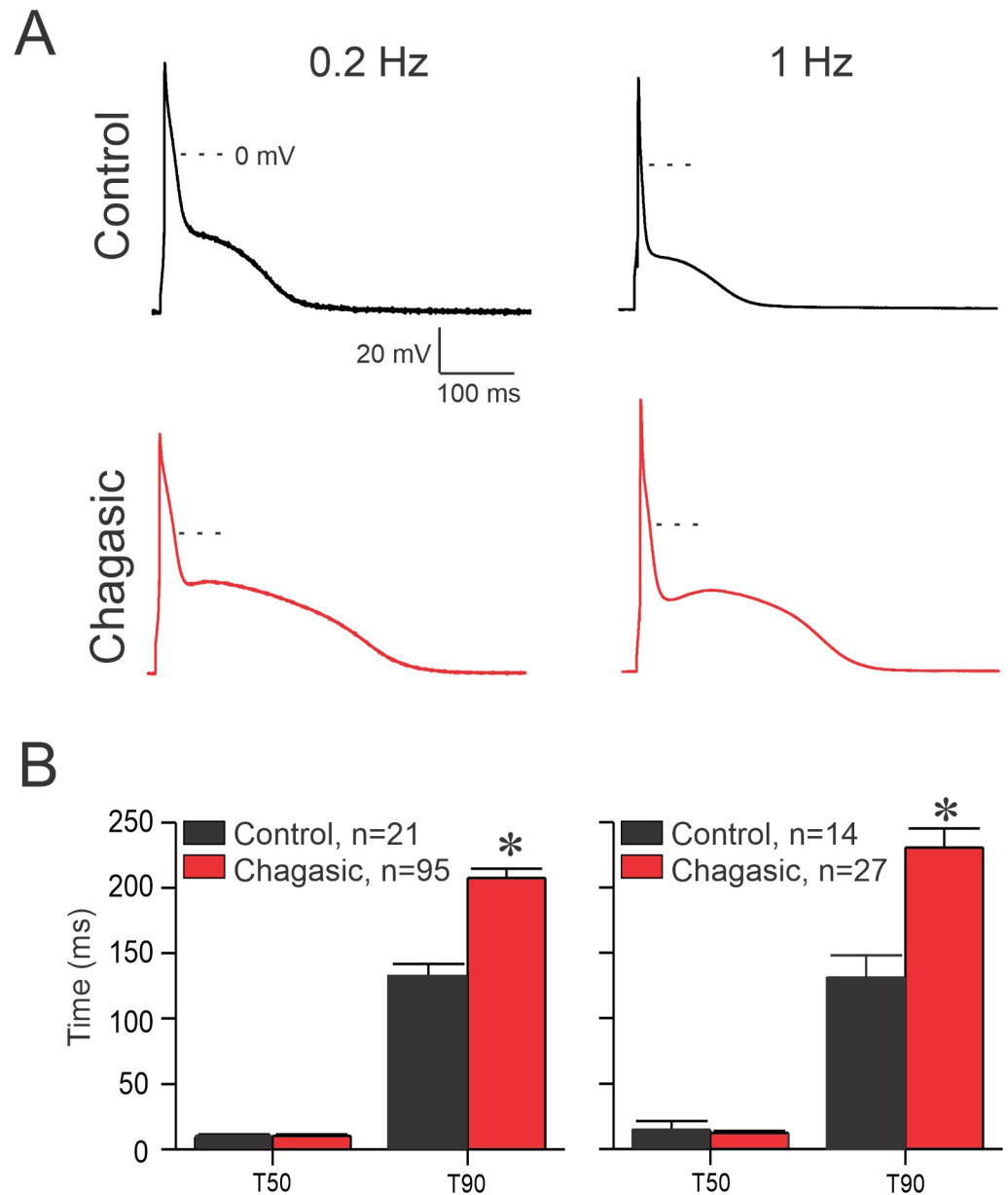


**Fig 1. Prolonged action potential (AP) duration in chagasic cardiomyocytes.** (A) Representative AP recorded from control (black traces) and infected (red traces) isolated cardiomyocytes paced at 0.2 Hz and 1 Hz. (B) Time required to 50% ( $T_{50}$ ) and 90% ( $T_{90}$ ) of full AP repolarization at 0.2 Hz and 1 Hz. Data were analyzed using Two-way ANOVA. n represents the number of cells. \* $p < 0.05$ .

<https://doi.org/10.1371/journal.pntd.0009421.g001>

### Isolated left ventricular cardiomyocytes from chagasic mice are more susceptible to spontaneous electrical activity

Fig 2A shows representative 8–9 consecutive APs from healthy and diseased LVCs paced at 0.2 and 1 Hz (top and bottom respectively). In Fig 2 AP instability (i.e early and delayed afterdepolarizations, both subthreshold or able to trigger spontaneous AP) is evident from chagasic LVC, as exemplified by colored arrows. Fig 2B shows the proportion of cells that presented AP instability. Only a minority (between 18% and 22% for 0.2 Hz and 1 Hz, respectively) of LVCs

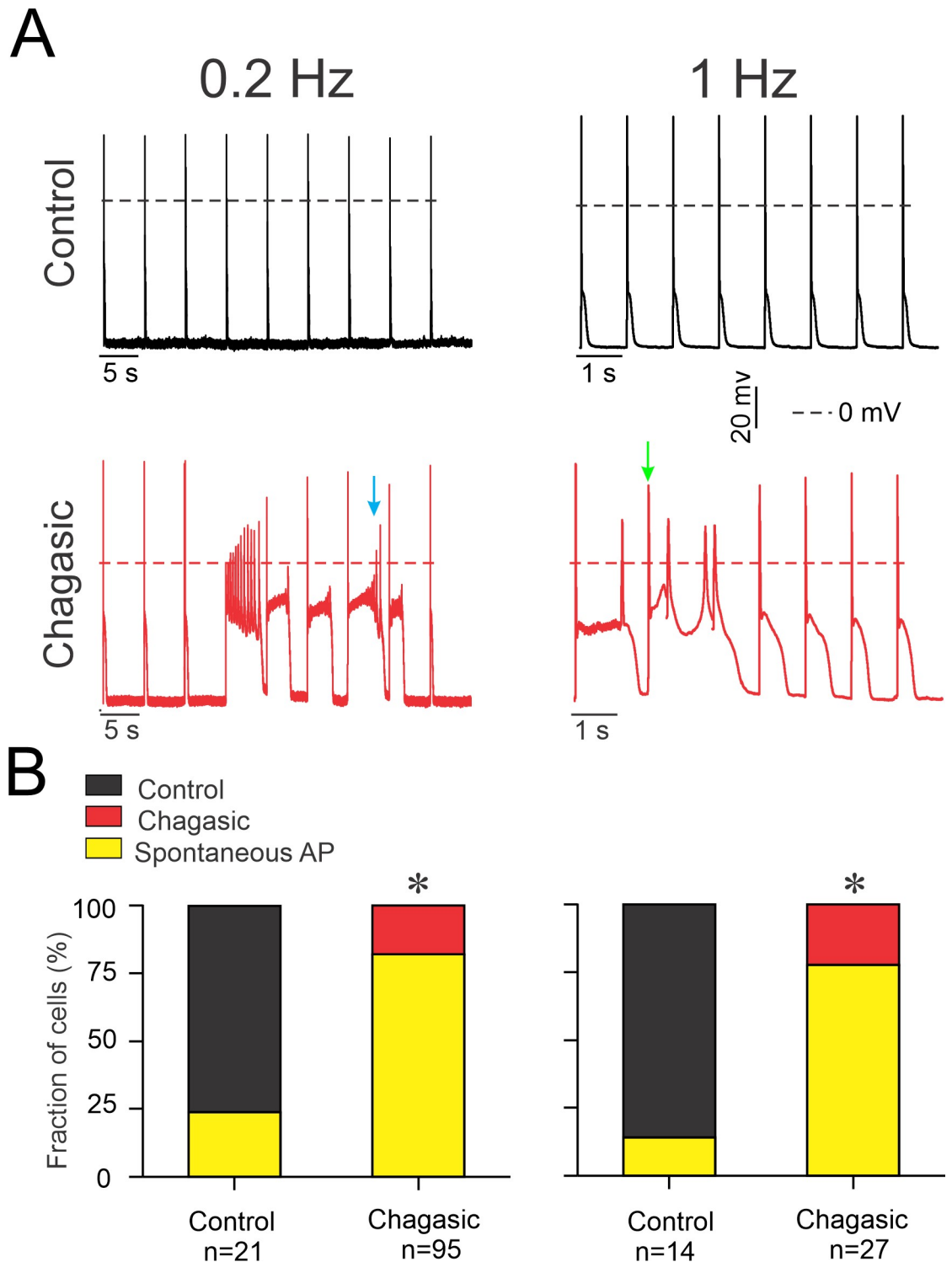


**Fig 2. Membrane potential instability due to after-depolarization events in the chronic phase of experimental Chagas disease.** (A) Eight to nine consecutive recorded action potentials from control and infected isolated cardiomyocytes paced at 0.2 Hz and 1 Hz. (B) The fraction of cells displaying membrane potential instability triggered by after-depolarizations, either during membrane repolarization (exemplified by the blue arrow) or after full membrane repolarization (exemplified by the green arrow). Data were compared using Fisher's exact test. n represents the number of cells. \*p<0.05.

<https://doi.org/10.1371/journal.pntd.0009421.g002>

from infected mice showed consistent AP morphology, while for control group the majority of cells (between 76% and 86% for 0.2 Hz and 1 Hz) showed regular AP morphology. In conclusion, LVC from chagasic mice are more susceptible to develop AP instabilities despite pacing frequency ( $p < 0.05$ ).

### **Ni<sup>2+</sup> and SEA0400 restore action potential properties in experimental Chagas disease**

There is a myriad of ionic mechanisms that could trigger AP instability, including  $I_{Na,L}$  [14, 15], T-type  $Ca^{2+}$  current [16], and  $I_{NCX}$  [17]. In order to evaluate the possible involvement of  $I_{NCX}$  in the electrical remodeling observed, we challenge cells prior and after exposure to  $Ni^{2+}$  (non-selective inhibitor of  $I_{NCX}$ ) and we monitored AP waveform. As depicted in Fig 3A, AP paced at 0.2 Hz from healthy LVCs are sensitive to 5 mM  $Ni^{2+}$  exposure. Importantly, when LVC from chagasic mice were exposed to 5 mM  $Ni^{2+}$  we observed a reduction of APR time taken at 90% repolarization ( $T_{90}$ ), as shown in Fig 3B. The mean fractional reduction of  $T_{90}$  of control and chagasic mice before and after exposure to  $Ni^{2+}$  is displayed in Fig 3C. These AP instabilities were reduced when perfusing  $Ni^{2+}$  on LVCs from chagasic mice [6,7,9,10]. Since  $Ni^{2+}$  is a non-selective inhibitor of  $I_{NCX}$  we performed the same experiment, however, challenging cells with SEA0400, which is considered a selective inhibitor of  $I_{NCX}$  [18]. As shown in Fig 4A, healthy and diseased LVC are sensitive to SEA0400. Interestingly, as quantified in Fig 4B, AP waveform from chagasic LVC was strongly affected by SEA0400, as measured by  $APR_{90\%}$ . After exposure of diseased LVC to SEA0400, AP duration was similar to that observed in the control group, which supports the hypothesis that  $I_{NCX}$  plays an important role in AP remodeling in CCM. Finally, the mean fractional reduction of  $T_{90}$  of control and chagasic mice before and after exposure to SEA0400 is displayed in Fig 4C.

### **Pause-induced transient inward current ( $I_{Ti}$ ) is augmented in chagasic cardiomyocytes and is sensitive to $Ni^{2+}$ and SEA0400**

There is evidence in the literature that enhanced  $I_{Ti}$  as a result of a stimulation regime of tachycardia following a pause is due to increased  $Ca^{2+}$  accumulation into the SR [19]. Thus, we decided to investigate whether  $I_{Ti}$  is increased in our experimental model of CD. Fig 5 summarizes our findings. When control and chagasic LVC were stimulated with either short or prolonged AP-like stimulation protocols, both chagasic and control cell groups displayed  $I_{Ti}$  but with distinct behavior (Fig 5A). It is important to note that a larger number of infected LVC presented  $I_{Ti}$  when compared to controls (Fig 5B and 5C). Also, the total  $I_{Ti}$  calculated was larger in infected when compared to control LVC (Fig 5D and 5E). In order to determine whether  $I_{Ti}$  is sensitive to  $Ni^{2+}$  and SEA0400 we ran the same protocol in another set of cells. First, we applied the protocol depicted on the top of Fig 6A which mimics the prolonged AP waveform typical from chagasic LVC, prior and after extracellular perfusion with 5 mM  $Ni^{2+}$ . As demonstrated in Fig 6B, the net  $I_{Ti}$  is substantially larger in chagasic LVC and it was attenuated to control level after 5 mM  $Ni^{2+}$  perfusion, meanwhile  $I_{Ti}$  in the control group is insensitive to 5mM of  $Ni^{2+}$ . A similar protocol was used for 1  $\mu$ M SEA0400 (Fig 7A) and a similar result was observed for SEA0400 (Fig 7B). Thus, with these experiments, we can conclude that chagasic LVC are more susceptible to generate  $I_{Ti}$  sensitive to  $Ni^{2+}$  and SEA0400.

### **Ion currents in experimental chronic Chagas disease**

In the literature it is well documented that  $I_{NCX}$  is sensitive to  $Ni^{2+}$  [17]. During the ramp protocol, the membrane potential was initially held at  $-30$  mV to inactivate  $Na^+$  channels. Cells

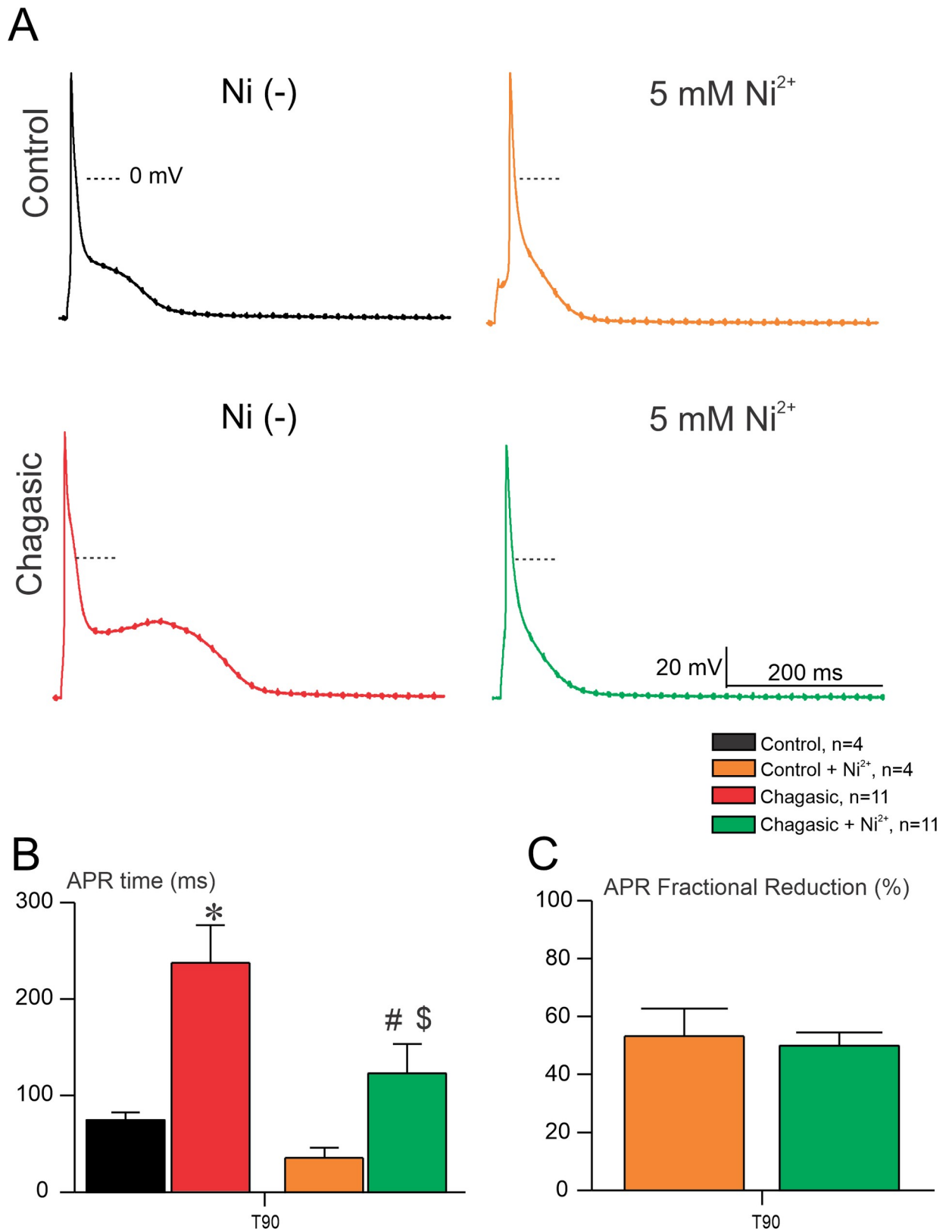


**Fig 3. Ni<sup>2+</sup> shortens action potential duration in chronic phase of experimental Chagas disease.** (A) Representative AP recorded from isolated cardiomyocytes from control and infected mice, before and after perfusion of Ni<sup>2+</sup> (5 mM). (B) Time required to reach 90% (T<sub>90</sub>) of full AP repolarization before and after exposure to Ni<sup>2+</sup> (5 mM). (C) AP repolarization (APR) fractional reduction taken at 90% after challenge control and chagasic cardiomyocytes with Ni<sup>2+</sup> at 5mM. Data were compared using one-way ANOVA (B) and Student's t test (C). n represents the number of cells. \* comparing Chagasic to control prior Ni<sup>2+</sup>, # comparing Chagasic prior and after Ni<sup>2+</sup>, \$ comparing Chagasic to control after Ni<sup>2+</sup> (p<0.05).

<https://doi.org/10.1371/journal.pntd.0009421.g003>

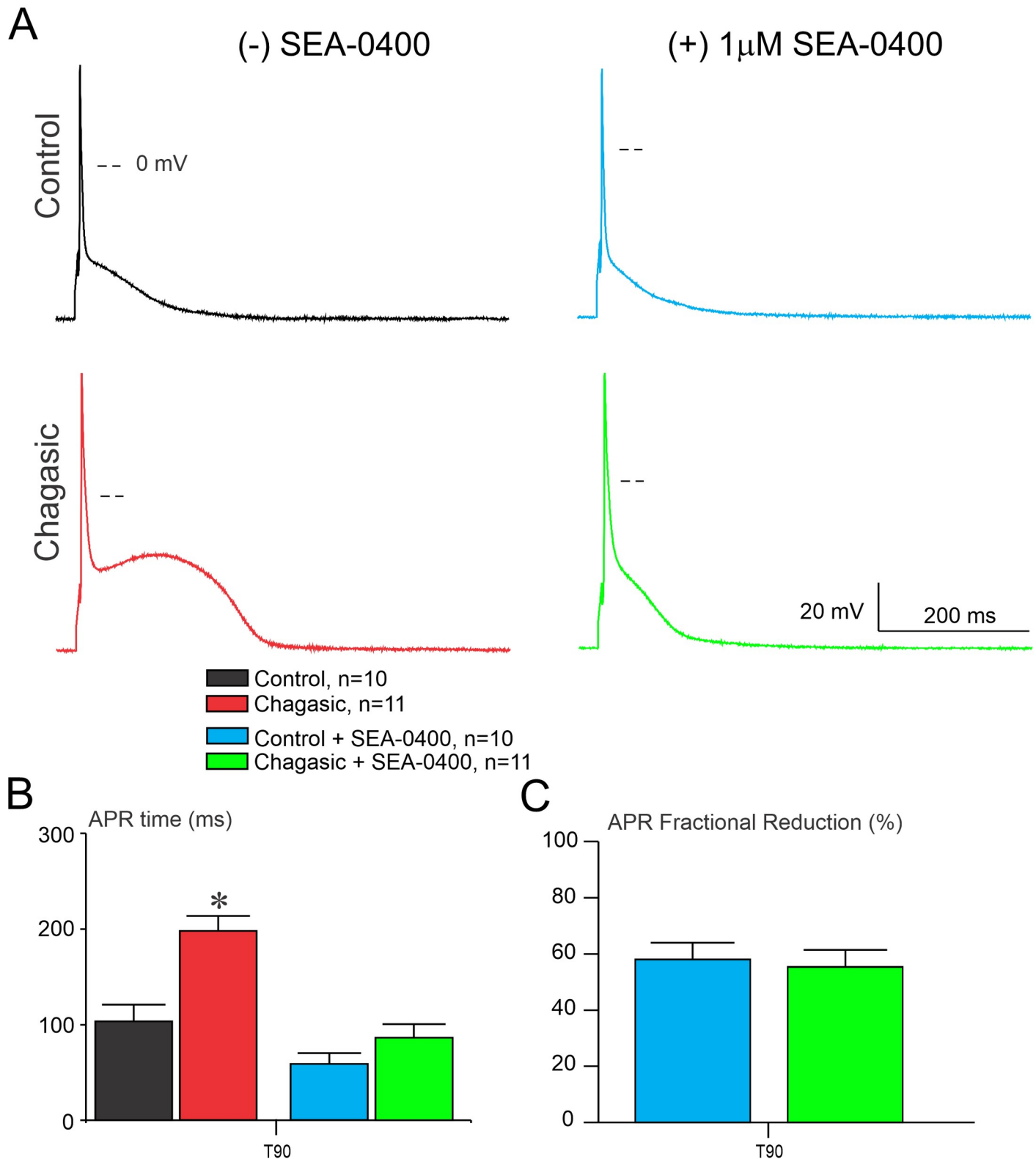


**Fig 4. SEA0400 shorts action potential waveform in the chronic phase of experimental Chagas disease.** (A) Representative AP recorded from cardiomyocytes isolated from control and infected mice, before and after perfusion of SEA0400 (1  $\mu$ M). (B) Time required to 90% ( $T_{90}$ ) of full AP repolarization before and after exposure to SEA0400 (1  $\mu$ M). (C) AP repolarization (APR) fractional reduction taken at 90% after challenge cells with SEA0400 (1  $\mu$ M). Data were compared using one-way ANOVA (B) and Student's t test (C). n represents the number of cells. \* comparing Chagasic without SEA0400 to all other groups ( $p < 0.05$ ).

<https://doi.org/10.1371/journal.pntd.0009421.g004>

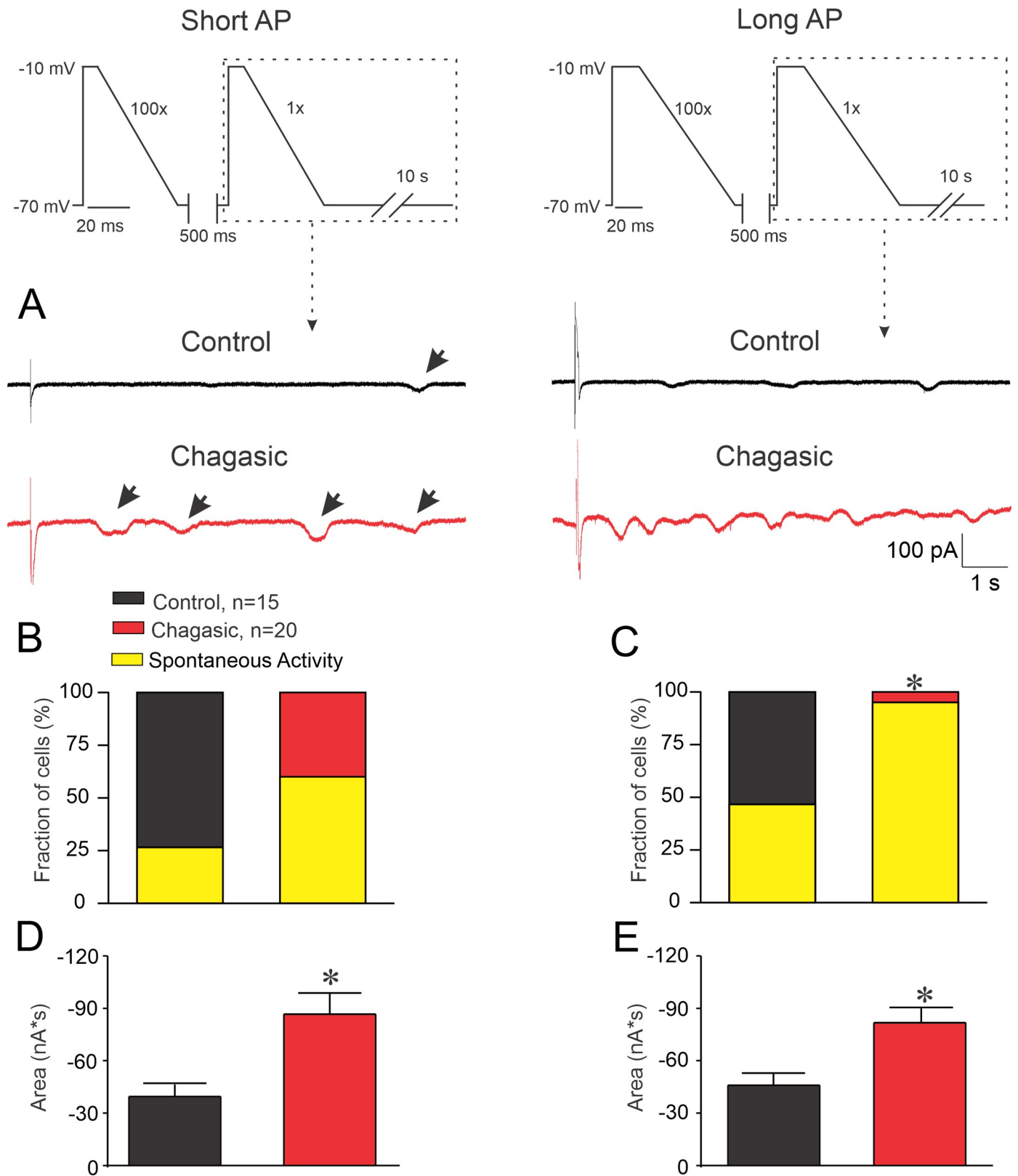


**Fig 5. Enhanced susceptibility for the appearance of transient inward current ( $I_{Ti}$ ) in the chronic phase of experimental Chagas disease.** The stimulation protocol is depicted at the top of the figure. (A) Current traces following 100 pre-conditioning pulses and a single 500 ms pause using a short pulse (left) and a long

pulse (right). Black arrows indicate  $I_{Ti}$ . (B) and (C) are the percentage of cells showing any identifiable  $I_{Ti}$ , using short and long pulses, respectively. (D) and (E) are bar graphs summarizing, only for those cells that developed  $I_{Ti}$ , the calculated integral of the  $I_{Ti}$  responses recorded with short and long pulses, respectively. Data were compared using Fisher's exact test (B and C) and Student's *t* test for (D and E). *n* represents the number of cells. \**p*<0.05.

<https://doi.org/10.1371/journal.pntd.0009421.g005>

were then depolarized to +40 mV to induce an outward current (reverse mode of NCX), as seen in Fig 8. The current becomes inward (forward mode of NCX) as the cell is hyperpolarized to -70 mV. The protocol was repeated in the presence of  $Ni^{2+}$  to yield what we defined as  $Ni^{2+}$ -sensitive current which was interpreted as  $I_{NCX}$ . Fig 8A shows representative tracings of  $I_{NCX}$  from control (left traces) and chagasic (right traces) LVC. The mean population data of peak outward current density (at +40 mV) reveals that  $I_{NCX}$  was similar in control and chagasic LVC (*p*>0.05). Also, as indicated by our analysis from -70 to +40 mV (Fig 8B) the net  $I_{NCX}$  is similar in control and chagasic LVC. In order to further explore this issue, we assessed  $Na^+$ / $Ca^{2+}$  exchanger activity in patch-clamped LVC by rapidly applying 10 mM caffeine to the bath solution while recording membrane current at a holding potential set at -80 mV. To ensure a steady SR loading, cells were pre-pulsed as indicated in the method section. In control LVC, the application of caffeine induced a large inward current, as depicted in Fig 9A (Top trace). However, in chagasic LVC, caffeine-induced inward current was significantly smaller (Fig 9A, Bottom trace). Fig 9B shows composite data. These functional data are consistent with reduced SR  $Ca^{2+}$  content as suggested in previous study [10]. Finally, using RT-PCR analysis and endogenous 18S mice for internal normalization, the detection of *T. cruzi* in isolated LVC from infected mice was demonstrated. The results of RT-PCR amplification of 18S *T. cruzi* are shown in Fig 10A, the threshold cycle (Fig 10B), and relative expression (Fig 10C).

## Discussion

Cardiac arrhythmia is a common trait in the chronic phase of CD and it is also a common finding in experimental murine models of CD [5,6,9]. Arrhythmias are determined by examination of the surface electrocardiogram that reveals, for instance, premature ventricular beats, sustained and non-sustained ventricular tachycardia, which may be attributed to altered cardiomyocyte excitability [19,20]. In the last decade, a substantial advance in the understanding of the cellular basis for ventricular arrhythmias in CD occurred, taking advantage of experimental animal models. However, major gaps in the field remain to be addressed. In the present investigation, we found a new cellular arrhythmogenic substrate in a murine model of CD, which can enable us to pursue new and more specific therapeutic approaches in future studies.

In previous studies using a murine model of CD, it was found profound alteration in cellular excitability of LVC during the time-course of the disease [6], and this was associated with the production of inflammatory cytokines [6,12]. Importantly it was described an AP prolongation that was linked to the reduction of voltage-dependent  $K^+$  currents [6,7]. In these previous studies, however, the use of  $Ca^{2+}$  chelator into the patch-clamp pipette during AP recordings probably diminished the surge of  $Ca^{2+}$ -dependent conductances in the AP waveform. This maneuver likely prevented the appearance of pro-arrhythmogenic events, such as after-depolarizations and could further underestimate the remodeling of AP waveform after *T. cruzi* infection. Thus, we decided to revisit the AP waveform, but now measuring it without adding a  $Ca^{2+}$  chelator into the patch-clamp pipette. Under these conditions, we did observe the appearance of afterdepolarizations that culminate in spontaneous AP, which could be triggered by  $I_{Ti}$  [19,21]. Also,  $I_{Ti}$  has long been recognized to be arrhythmogenic, underlying transient membrane depolarizations in conditions of intracellular  $Ca^{2+}$  overload [19,22].  $I_{Ti}$  is dependent on intracellular  $Ca^{2+}$  concentration [23,24], a condition that we have previously shown to be increased in cardiomyocytes isolated from chagasic mice in the acute phase (30–

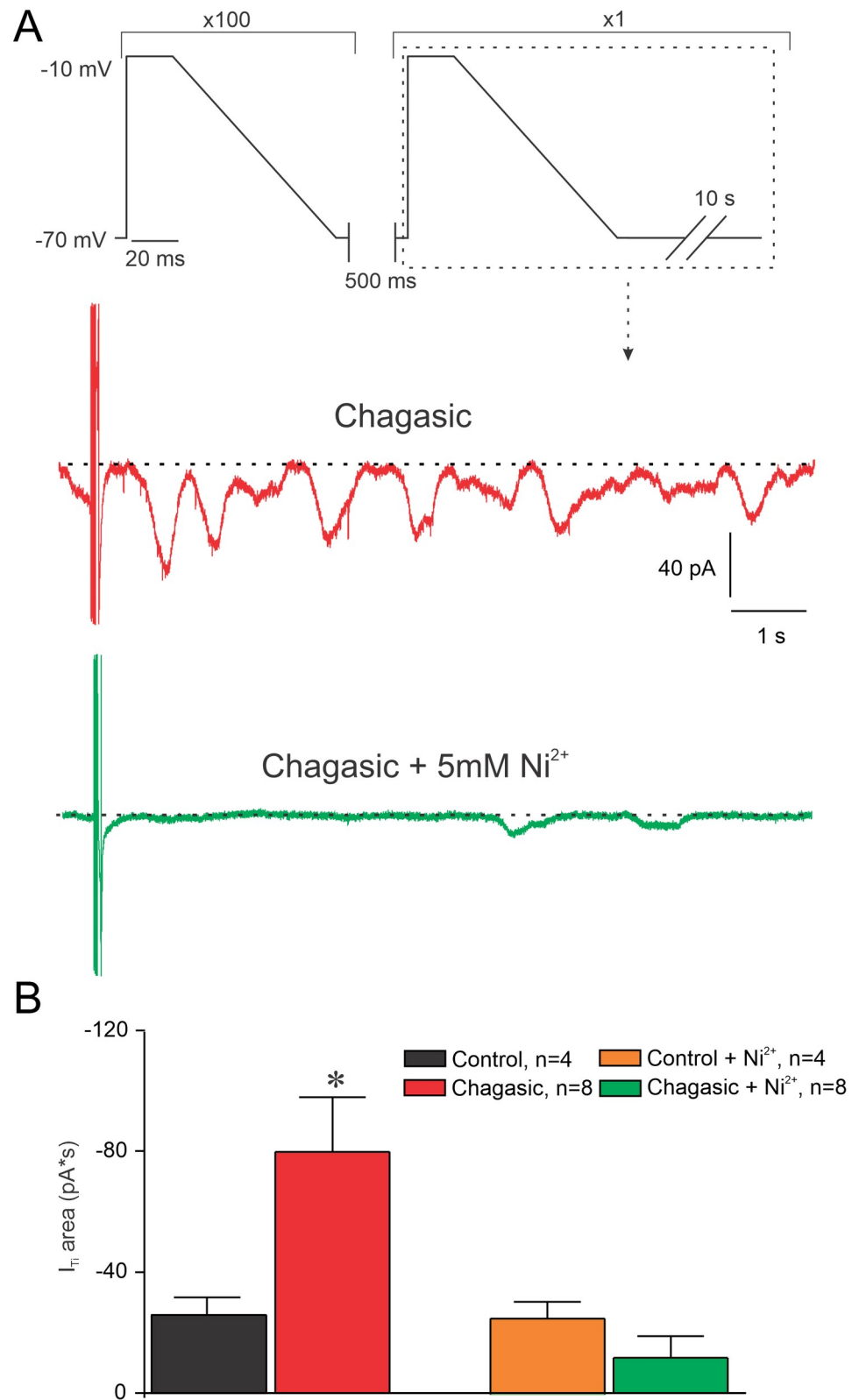


**Fig 6. Ni<sup>2+</sup> attenuates transient inward current (I<sub>Tr</sub>) in the chronic phase of experimental Chagas disease.** The protocol is depicted at the top of the figure. (A) Current traces following 100 pre-conditioning pulses and a single 500 ms pause using long pulse, before (red) and after perfusion of 5 mM Ni<sup>2+</sup> (green traces). (B) Composite data

representing the calculated area during  $I_{Ti}$  responses recorded from isolated cardiomyocytes from control and infected mice using long AP-simulating pulses, before and after  $Ni^{2+}$  perfusion. Data were compared using OneWay ANOVA.  $n$  represents the number of cells. \* $p < 0.05$ .

<https://doi.org/10.1371/journal.pntd.0009421.g006>

45 days post-infection [9]). In line with this idea, diastolic  $Ca^{2+}$  overload is also a hallmark of cardiomyocytes from humans with CCM [25].

In order to better explore the role of APR prolongation in arrhythmogenesis in LVC we simulated two situations for both groups of cells: a train of AP-like voltage-clamp with (1) control and (2) chagasic features. By using the first simulated condition we observed that a greater number of chagasic LVC developed  $I_{Ti}$  showing larger amplitude when compared to controls. For the second simulated condition, we continued to observe a greater number of chagasic LVC developing  $I_{Ti}$  when compared to controls. Combined these results indicate that only rescuing AP waveform may be not enough to prevent arrhythmogenesis in CD.

On the other hand, reduction of AP duration and membrane potential instabilities were observed when chagasic LVC were exposed to  $Ni^{2+}$ . Thus,  $Ni^{2+}$  likely does both reduce AP prolongation and attenuate  $I_{Ti}$ . It is well known that  $Ni^{2+}$  is used to study  $Na^+/Ca^{2+}$  exchanger function in cardiomyocytes [26,27]. However, it is relevant mentioning that  $Ni^{2+}$  can have off-target effects on ionic conductances other than the blockage of  $Na^+/Ca^{2+}$  exchanger with variable selectivity, including the blockage of  $Na^+$  current [28], and of several types of  $Ca^{2+}$  current, with higher affinity for T-type compared to L-type  $Ca^{2+}$  channels [29–31].  $Ca^{2+}$  dynamics has an important participation in shaping AP waveform and can be an important determinant of arrhythmogenic profile such as AP alternans [32]. Hence, the off-target effects of  $Ni^{2+}$  could be overestimating the contribution of  $Na^+/Ca^{2+}$  exchanger on remodeled AP from chagasic mice.

Nevertheless, our findings were further supported using a selective blocker of  $I_{NCX}$ , SEA0400. To our surprise,  $I_{NCX}$  density was comparable in both studied groups. It is worth to mention that in  $I_{NCX}$  recordings,  $[Ca^{2+}]_i$  was maintained at 152 nM, which excluded the modulatory effect of  $Na^+/Ca^{2+}$  exchanger by  $[Ca^{2+}]_i$  [33]. However, an increase in LVC diastolic  $[Ca^{2+}]_i$  as previously described by our group in chagasic mice [9], and in humans with CD [25], may lead to  $I_{NCX}$  activation [34], accounting for the observed prolongation of AP duration at more negative membrane potentials. It is important to note that using both blockers,  $Ni^{2+}$  and SEA0400, the fractional shortening of APR duration at T90 was similar in both, control and chagasic LVC. The result may suggest that prolongation of AP duration, as a consequence of reduced transient inward potassium current, as already reported in previous studies [7,8,10], favors enhanced contribution of  $I_{NCX}$  without increasing its current density. Further experiments are necessary to clarify this question.

Our results also point towards a reduction of SR  $Ca^{2+}$  load, as indicated by the reduction of caffeine-induced  $Ca^{2+}$  release from SR. This is in accordance with previous findings of reduced SERCA2A activity extrapolated from global  $Ca^{2+}$  transient decay time [6,10]. In this study, we strengthened the idea that  $Ca^{2+}$  dynamics dysfunction has an important role in the electrical remodeling of cardiomyocytes during experimental CD, as it was previously implicated in cardiomyocytes isolated from patients with CD [25]. The tachycardia-like protocol favors  $Ca^{2+}$  release from SR and, along with reduced SERCA2A function, would contribute to  $Ca^{2+}$  accumulation in the sarcoplasm. In the end, a prolonged AP in chagasic LVC elicited an increase in  $I_{NCX}$  at the diastolic level, explaining the fact that  $Ni^{2+}$  and SEA0400 reduced the pause-induced diastolic  $I_{Ti}$ . Lastly, since the molecular identification of *T. cruzi* in isolated LVC from chagasic mice was found, we may speculate that parasite persistence in the heart is an important component to the development of CCM, which would favor a chronic inflammation in

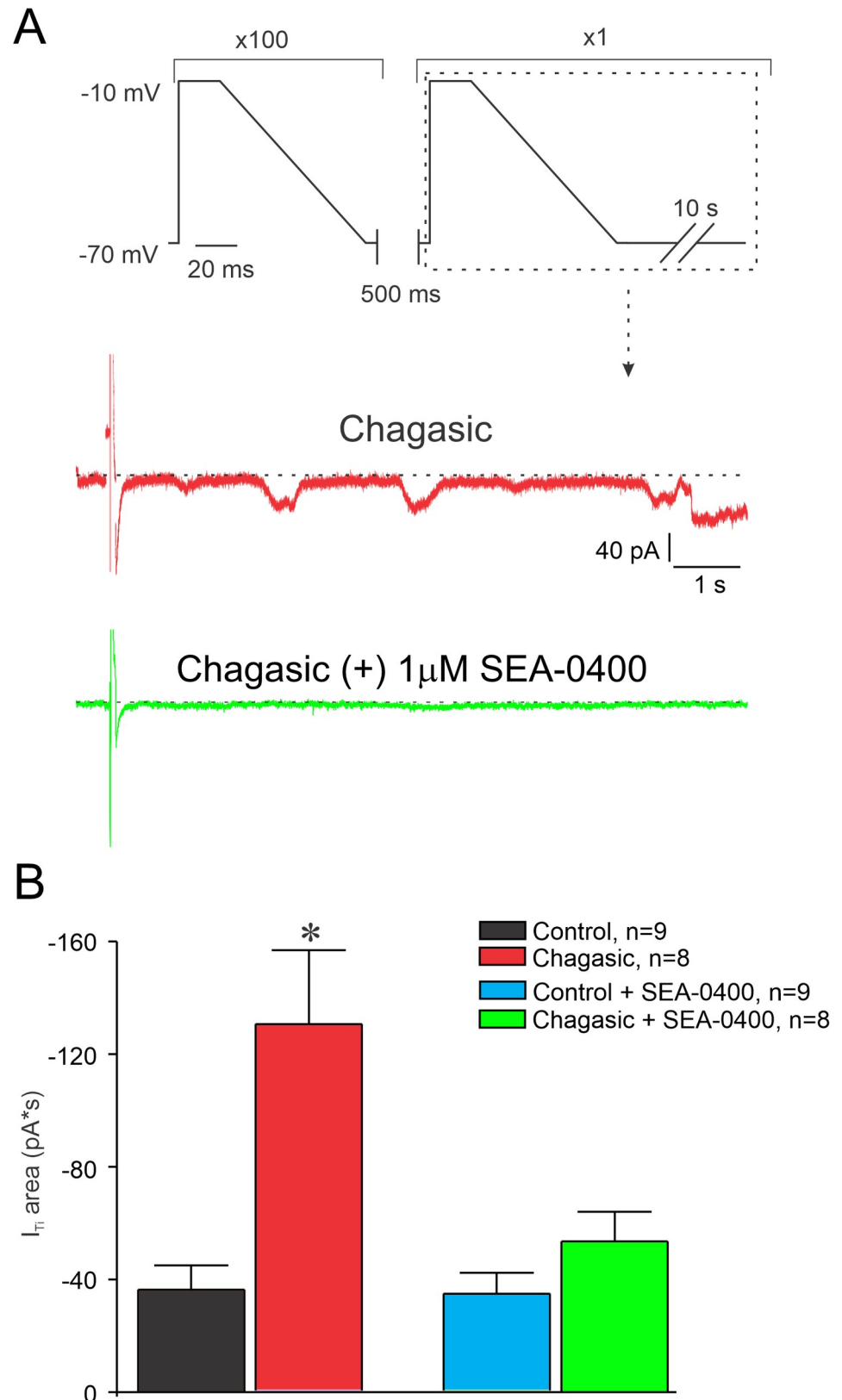


**Fig 7. SEA0400 attenuates transient inward current (IT<sub>1</sub>) in the chronic phase of experimental Chagas disease.** The protocol is depicted at the top of the figure. (A) Current traces following 100 pre-conditioning pulses and a single 500 ms pause using long pulse, before (red) and after perfusion of SEA0400 (1 µM). (B) Composite data representing the calculated integral of the IT<sub>1</sub> responses recorded from isolated cardiomyocytes from control and infected mice using

long pulses, before and after SEA0400 (1  $\mu$ M). Data were compared using OneWay ANOVA. n represents the number of cells. \* $p < 0.05$ .

<https://doi.org/10.1371/journal.pntd.0009421.g007>

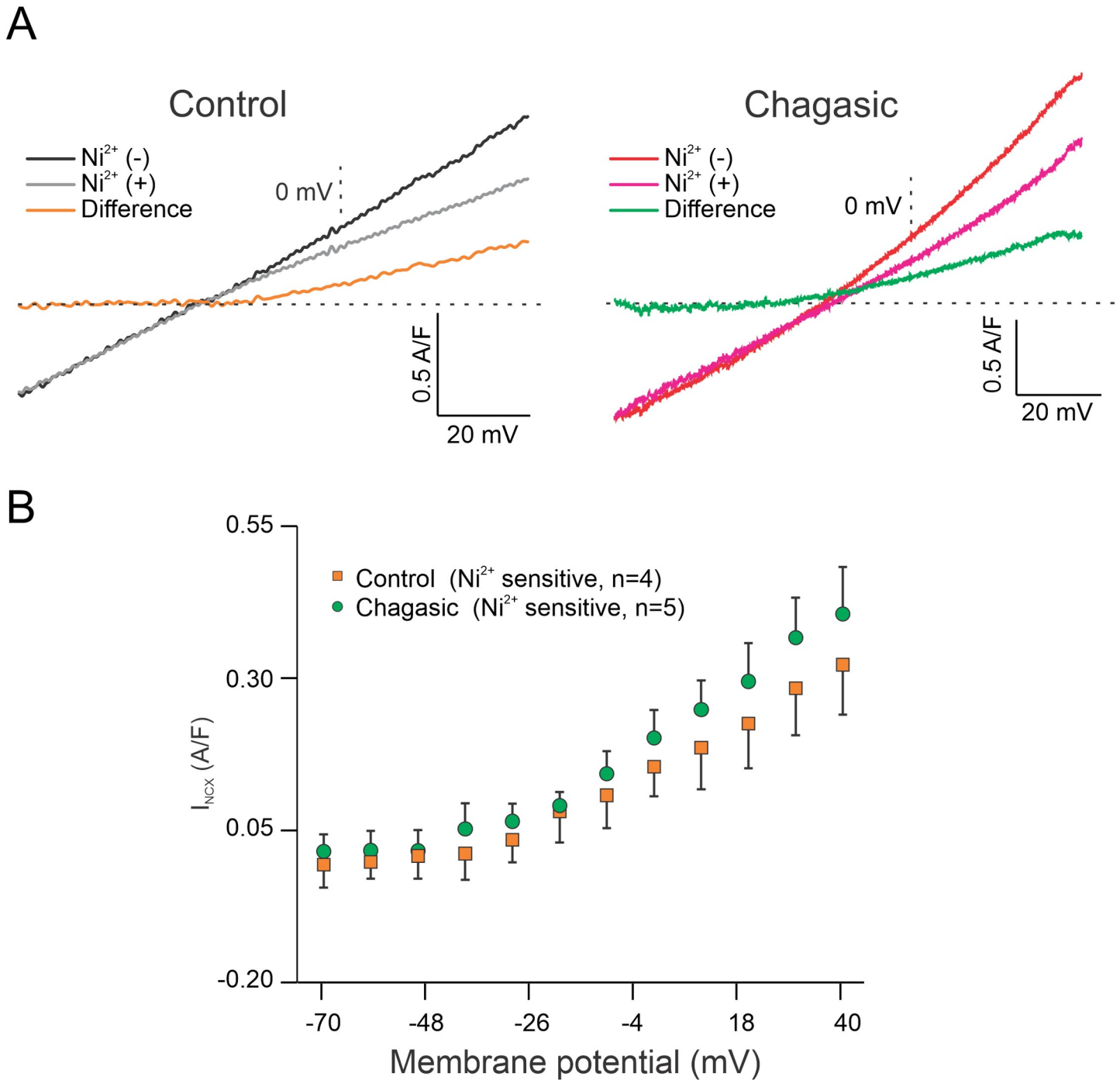


**Fig 8.  $\text{Ni}^{2+}$ -sensitive  $\text{Na}^+/\text{Ca}^{2+}$  exchange current ( $I_{\text{NCX}}$ ) density does not change in experimental Chagas disease.** (A) Representative  $I_{\text{NCX}}$  vs. Membrane Potential relationships before ( $\text{Ni}^{2+}$  (-)) and after ( $\text{Ni}^{2+}$  (+)) perfusion of 5 mM  $\text{Ni}^{2+}$  measured in isolated cardiomyocytes from control (Panel A, left) and infected (Panel A, right) mice. Orange and green traces represent the difference current obtained by digitally subtracting traces before and after  $\text{Ni}^{2+}$  application. (B) Average  $\text{Ni}^{2+}$ -subtracted Current Density versus Membrane Potential in control (orange squares) and chagasic (green circles) cardiomyocytes were not different. Data were analyzed using Two-way ANOVA. n indicates the number of cells.

<https://doi.org/10.1371/journal.pntd.0009421.g008>

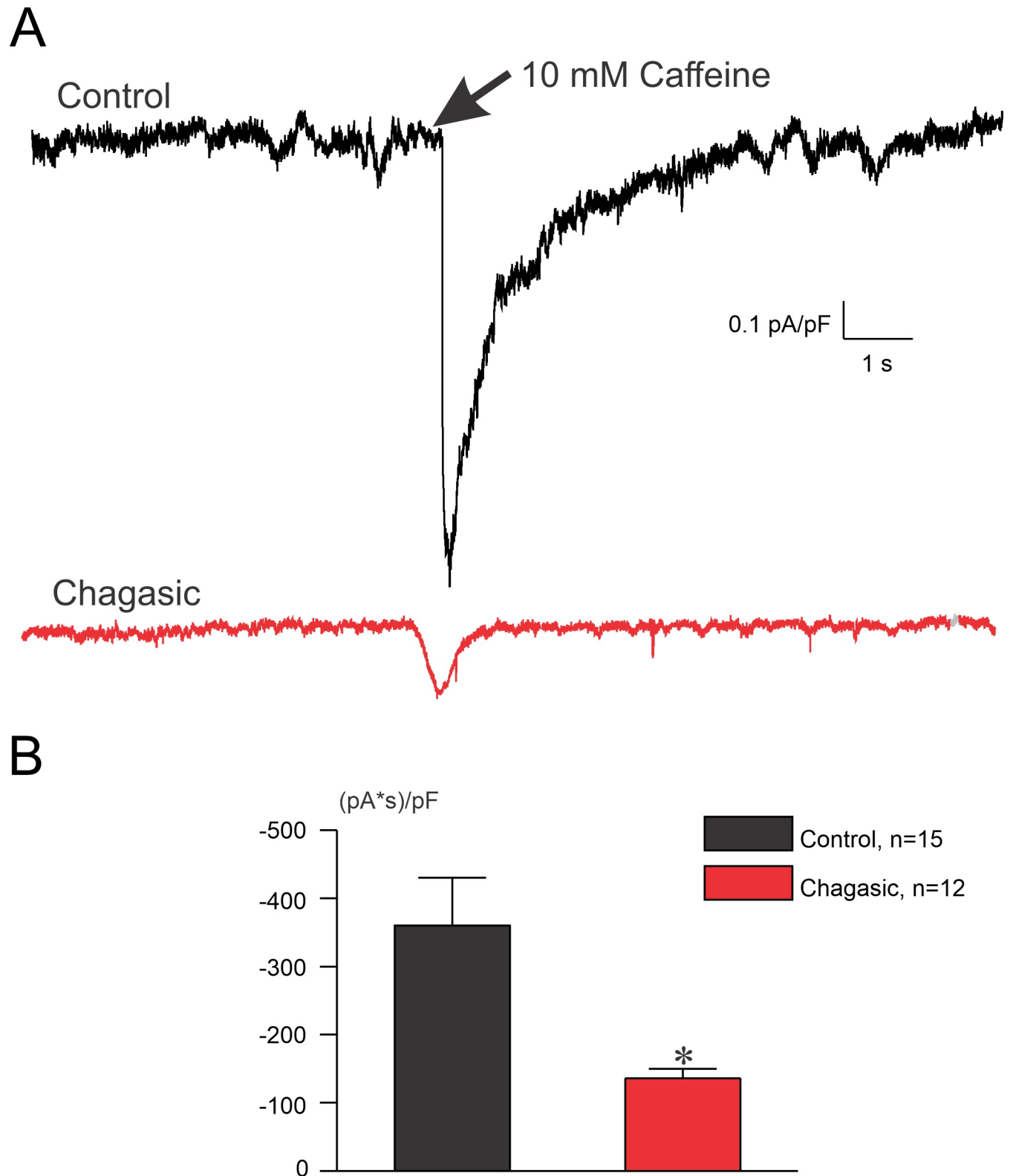


**Fig 9. Reduced sarcoplasmic reticulum  $\text{Ca}^{2+}$  content measured by  $\text{Na}^+/\text{Ca}^{2+}$  exchange current in the chronic phase of experimental Chagas disease.** (A) Representative recordings of caffeine-induced  $\text{Na}^+/\text{Ca}^{2+}$  exchange current ( $I_{\text{NCX}}$ ) in cardiomyocytes from control (black) and infected (red) mice. (B) Area of inward current measured in the presence of 10 mM caffeine. Data were compared using Student's t test. n indicates the number of cells. \* $p < 0.05$ .

<https://doi.org/10.1371/journal.pntd.0009421.g009>

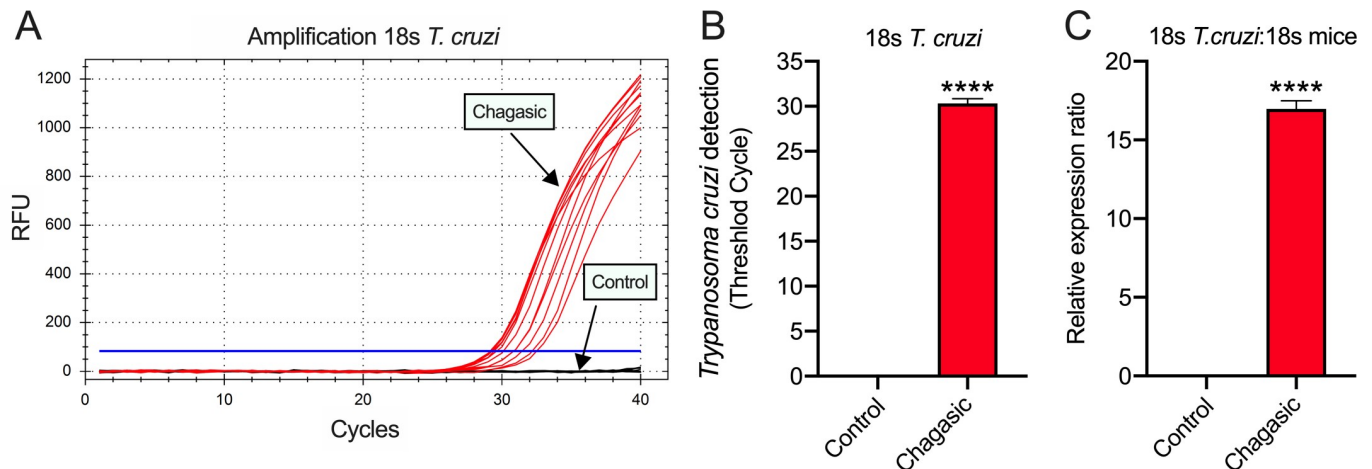


**Fig 10. Detection of *T. cruzi* in isolated left ventricular cardiomyocytes from mice.** RT-PCR analysis was performed using isolated cells obtained from mice 180 to 200 days after infection and age matched controls. The results of RT-PCR amplification of 18S *T. cruzi* (A), threshold cycle (B), and relative expression (C, represented as  $\Delta C_t$  values) were demonstrated. Data were normalized to mice 18S endogenous (isolated left ventricular cardiomyocytes).  $N = 5$  for both groups. Data were compared using Student's *t* test. \*\*\*\* $p < 0.0001$ .

<https://doi.org/10.1371/journal.pntd.0009421.g010>

the tissue, and then contribute to the observed electrical remodeling observed [35–37]. Future experiments are needed to access the putative association between parasite persistence and electrical remodeling in experimental CCM.

## Conclusion

In the present study, we demonstrate that in the chronic phase of experimental infection with *Trypanosoma cruzi* (TcI, Colombian strain), LVCs have increased AP duration and they are more susceptible to display early and delayed after-depolarizations, leading to increased frequency of cells showing spontaneous AP. Moreover, diseased LVCs are more prone to present pause-induced  $I_{Ti}$ . Most importantly, the arrhythmogenic mechanisms underlying these events are sensitive to  $Ni^{2+}$  and SEA0400, which certainly indicates the involvement of  $I_{NCX}$ . Thus, inhibiting  $I_{NCX}$  could be a potential and promising therapeutic strategy for the prevention of ventricular arrhythmias found in Chagasic cardiomyopathy.

## Study limitations

First, we conducted our cellular electrophysiological experiment at room temperature. Thus, the extrapolation of  $Ca^{2+}$  dynamics influence *in vivo* is limited. Second, we speculate that off-target effects of  $Ni^{2+}$  other than a block of  $I_{NCX}$  may also contribute to the antiarrhythmic effect. Also, we did not access the fraction of cardiomyocytes infected or not with *T. cruzi*, since cellular electrical remodeling was investigated as a result of the net heart impairment after chronic infection with *T. cruzi*. Further studies are necessary to resolve these issues.

## Supporting information

### S1 Table. Solutions used in patch-clamp experiments.

(DOCX)

### S2 Table. Action potential parameters.

(DOCX)

**S1 Data. Underlying data for the reported findings.**  
(XLSX)

## Author Contributions

**Conceptualization:** Artur Santos-Miranda, Danilo Roman-Campos.

**Data curation:** Danilo Roman-Campos.

**Formal analysis:** Artur Santos-Miranda, Allysson T. C. Soares, Danilo Roman-Campos.

**Funding acquisition:** Fabiana S. Machado, Jader S. Cruz, Danilo Roman-Campos.

**Investigation:** Artur Santos-Miranda, Julliane V. Joviano-Santos, Jaqueline O. Sarmento, Alexandre D. Costa, Allysson T. C. Soares, Danilo Roman-Campos.

**Methodology:** Artur Santos-Miranda.

**Supervision:** Jader S. Cruz, Danilo Roman-Campos.

**Writing – original draft:** Artur Santos-Miranda, Jader S. Cruz, Danilo Roman-Campos.

**Writing – review & editing:** Allysson T. C. Soares, Fabiana S. Machado, Jader S. Cruz, Danilo Roman-Campos.

## References

1. WHO. Fact sheets-Chagas disease. World Health Organization. 2020: 1.
2. Manne-Goehler J, Umeh CA, Montgomery SP, Wirtz VJ. Estimating the Burden of Chagas Disease in the United States. *PLoS neglected tropical diseases*. 2016; 10(11):e0005033. <https://doi.org/10.1371/journal.pntd.0005033> PMID: 27820837; PubMed Central PMCID: PMC5098725.
3. Kuehn BM. Chagas Heart Disease an Emerging Concern in the United States. *Circulation*. 2016; 134(12):895–6. <https://doi.org/10.1161/CIRCULATIONAHA.116.024839> PMID: 27647298.
4. Nunes MC, Dones W, Morillo CA, Encina JJ, Ribeiro AL, Council on Chagas Disease of the Interamerican Society of C. Chagas disease: an overview of clinical and epidemiological aspects. *Journal of the American College of Cardiology*. 2013; 62(9):767–76. <https://doi.org/10.1016/j.jacc.2013.05.046> PMID: 23770163.
5. Marin-Neto JA, Cunha-Neto E, Maciel BC, Simoes MV. Pathogenesis of chronic Chagas heart disease. *Circulation*. 2007; 115(9):1109–23. <https://doi.org/10.1161/CIRCULATIONAHA.106.624296> PMID: 17339569.
6. Roman-Campos D, Sales-Junior P, Duarte HL, Gomes ER, Lara A, Campos P, et al. Novel insights into the development of chagasic cardiomyopathy: role of PI3Kinase/NO axis. *International journal of cardiology*. 2013; 167(6):3011–20. <https://doi.org/10.1016/j.ijcard.2012.09.020> PMID: 23031286.
7. Cruz JS, Santos-Miranda A, Sales-Junior PA, Monti-Rocha R, Campos PP, Machado FS, et al. Altered Cardiomyocyte Function and Trypanosoma cruzi Persistence in Chagas Disease. *The American journal of tropical medicine and hygiene*. 2016; 94(5):1028–33. <https://doi.org/10.4269/ajtmh.15-0255> PMID: 26976879; PubMed Central PMCID: PMC4856598.
8. Pacioretty LM, Barr SC, Han WP, Gilmour RF Jr. Reduction of the transient outward potassium current in a canine model of Chagas' disease. *The American journal of physiology*. 1995; 268(3 Pt 2):H1258–64. Epub 1995/03/11. <https://doi.org/10.1152/ajpheart.1995.268.3.H1258> PMID: 7900880.
9. Santos-Miranda A, Joviano-Santos JV, Ribeiro GA, Botelho AFM, Rocha P, Vieira LQ, et al. Reactive oxygen species and nitric oxide imbalances lead to in vivo and in vitro arrhythmogenic phenotype in acute phase of experimental Chagas disease. *PLoS pathogens*. 2020; 16(3):e1008379. Epub 2020/03/12. <https://doi.org/10.1371/journal.ppat.1008379> PMID: 32160269; PubMed Central PMCID: PMC7089563.
10. Roman-Campos D, Sales-Junior P, Duarte HL, Gomes ER, Guatimosim S, Ropert C, et al. Cardiomyocyte dysfunction during the chronic phase of Chagas disease. *Memorias do Instituto Oswaldo Cruz*. 2013; 108(2):243–5. <https://doi.org/10.1590/0074-0276108022013019> PMID: 23579807; PubMed Central PMCID: PMC3970661.

11. Duz AL, Vieira PM, Roatt BM, Aguiar-Soares RD, Cardoso JM, Oliveira FC, et al. The TcI and TcII Trypanosoma cruzi experimental infections induce distinct immune responses and cardiac fibrosis in dogs. *Memorias do Instituto Oswaldo Cruz*. 2014; 109(8):1005–13. Epub 2015/01/16. <https://doi.org/10.1590/0074-02760140208> PMID: 25591108; PubMed Central PMCID: PMC4325618.
12. Roman-Campos D, Duarte HL, Sales PA Jr., Natali AJ, Ropert C, Gazzinelli RT, et al. Changes in cellular contractility and cytokines profile during Trypanosoma cruzi infection in mice. *Basic Res Cardiol*. 2009; 104(3):238–46. <https://doi.org/10.1007/s00395-009-0776-x> PMID: 19190953.
13. Shioya T. A simple technique for isolating healthy heart cells from mouse models. *J Physiol Sci*. 2007; 57(6):327–35. <https://doi.org/10.2170/physiolsci.RP010107> WOS:000252934300001. PMID: 17980092
14. Iyer V, Roman-Campos D, Sampson KJ, Kang G, Fishman GI, Kass RS. Purkinje Cells as Sources of Arrhythmias in Long QT Syndrome Type 3. *Scientific reports*. 2015; 5:13287. <https://doi.org/10.1038/srep13287> PMID: 26289036; PubMed Central PMCID: PMC4542521.
15. Zhang Q, Ma JH, Li H, Wei XH, Zheng J, Li G, et al. Increase in CO2 levels by upregulating late sodium current is proarrhythmic in the heart. *Heart Rhythm*. 2019; 16(7):1098–106. <https://doi.org/10.1016/j.hrthm.2019.01.029> PMID: 30710739.
16. Cribbs L. T-type calcium channel expression and function in the diseased heart. *Channels*. 2010; 4(6):447–52. <https://doi.org/10.4161/chan.4.6.12870> PMID: 21139421.
17. Bogeholz N, Pauls P, Bauer BK, Schulte JS, Dechering DG, Frommeyer G, et al. Suppression of Early and Late Afterdepolarizations by Heterozygous Knockout of the Na<sup>+</sup>/Ca<sup>2+</sup> Exchanger in a Murine Model. *Circulation Arrhythmia and electrophysiology*. 2015; 8(5):1210–8. <https://doi.org/10.1161/CIRCEP.115.002927> PMID: 26338832.
18. Iwamoto T, Watanabe Y, Kita S, Blaustein MP. Na<sup>+</sup>/Ca<sup>2+</sup> exchange inhibitors: a new class of calcium regulators. *Cardiovascular & hematological disorders drug targets*. 2007; 7(3):188–98. Epub 2007/09/28. <https://doi.org/10.2174/187152907781745288> PMID: 17896959.
19. Lindegger N, Hagen BM, Marks AR, Lederer WJ, Kass RS. Diastolic transient inward current in long QT syndrome type 3 is caused by Ca<sup>2+</sup> overload and inhibited by ranolazine. *Journal of molecular and cellular cardiology*. 2009; 47(2):326–34. Epub 2009/04/18. <https://doi.org/10.1016/j.yjmcc.2009.04.003> PMID: 19371746; PubMed Central PMCID: PMC2703681.
20. Matthews GD, Guzhadur L, Sabir IN, Grace AA, Huang CL. Action potential wavelength restitution predicts alternans and arrhythmia in murine Scn5a(+/-) hearts. *The Journal of physiology*. 2013; 591(17):4167–88. <https://doi.org/10.1113/jphysiol.2013.254938> PMID: 23836691; PubMed Central PMCID: PMC3779110.
21. Fredj S, Lindegger N, Sampson KJ, Carmeliet P, Kass RS. Altered Na<sup>+</sup> channels promote pause-induced spontaneous diastolic activity in long QT syndrome type 3 myocytes. *Circulation research*. 2006; 99(11):1225–32. <https://doi.org/10.1161/01.RES.0000251305.25604.b0> PMID: 17082480; PubMed Central PMCID: PMC4454351.
22. Lederer WJ, Tsien RW. Transient inward current underlying arrhythmogenic effects of cardiotonic steroids in Purkinje fibres. *The Journal of physiology*. 1976; 263(2):73–100. <https://doi.org/10.1113/jphysiol.1976.sp011622> PMID: 1018270; PubMed Central PMCID: PMC1307691.
23. Kass RS, Tsien RW. Fluctuations in membrane current driven by intracellular calcium in cardiac Purkinje fibers. *Biophys J*. 1982; 38(3):259–69. [https://doi.org/10.1016/S0006-3495\(82\)84557-8](https://doi.org/10.1016/S0006-3495(82)84557-8) PMID: 6809065; PubMed Central PMCID: PMC1328867.
24. Kass RS, Lederer WJ, Tsien RW, Weingart R. Role of calcium ions in transient inward currents and aftercontractions induced by strophanthidin in cardiac Purkinje fibres. *The Journal of physiology*. 1978; 281:187–208. <https://doi.org/10.1113/jphysiol.1978.sp012416> PMID: 702368; PubMed Central PMCID: PMC1282691.
25. Mijares A, Espinosa R, Adams J, Lopez JR. Increases in [IP3]i aggravates diastolic [Ca<sup>2+</sup>] and contractile dysfunction in Chagas' human cardiomyocytes. *PLoS neglected tropical diseases*. 2020; 14(4): e0008162. Epub 2020/04/11. <https://doi.org/10.1371/journal.pntd.0008162> PMID: 32275663; PubMed Central PMCID: PMC7176279.
26. Zeng B, Liao X, Liu L, Ruan H, Zhang C. Thyroid Hormone Diminishes Ca<sup>2+</sup> Overload Induced by Hypoxia/Reoxygenation in Cardiomyocytes by Inhibiting Late Sodium Current and Reverse-Na<sup>+</sup>/Ca<sup>2+</sup> Exchange Current. *Pharmacology*. 2020; 105(1–2):63–72. <https://doi.org/10.1159/000502804> PMID: 31514184.
27. Reppel M, Fleischmann BK, Reuter H, Sasse P, Schunkert H, Hescheler J. Regulation of the Na<sup>+</sup>/Ca<sup>2+</sup> exchanger (NCX) in the murine embryonic heart. *Cardiovascular research*. 2007; 75(1):99–108. <https://doi.org/10.1016/j.cardiores.2007.03.018> PMID: 17462611.
28. Sheets MF, Hanck DA. Mechanisms of extracellular divalent and trivalent cation block of the sodium current in canine cardiac Purkinje cells. *The Journal of physiology*. 1992; 454:299–320. Epub 1992/08/

01. <https://doi.org/10.1113/jphysiol.1992.sp019265> PMID: 1335503; PubMed Central PMCID: PMC1175606.
29. Perez-Reyes E. Molecular physiology of low-voltage-activated t-type calcium channels. *Physiological reviews*. 2003; 83(1):117–61. Epub 2002/12/31. <https://doi.org/10.1152/physrev.00018.2002> PMID: 12506128.
  30. Hobai IA, Hancox JC, Levi AJ. Inhibition by nickel of the L-type Ca channel in guinea pig ventricular myocytes and effect of internal cAMP. *American journal of physiology Heart and circulatory physiology*. 2000; 279(2):H692–701. Epub 2000/08/03. <https://doi.org/10.1152/ajpheart.2000.279.2.H692> PMID: 10924068.
  31. Ju YK, Allen DG. The mechanisms of sarcoplasmic reticulum Ca<sup>2+</sup> release in toad pacemaker cells. *The Journal of physiology*. 2000; 525 Pt 3(Pt 3):695–705. Epub 2000/06/16. <https://doi.org/10.1111/j.1469-7793.2000.t01-1-00695.x> PMID: 10856122; PubMed Central PMCID: PMC2269965.
  32. Kanaporis G, Blatter LA. The mechanisms of calcium cycling and action potential dynamics in cardiac alternans. *Circulation research*. 2015; 116(5):846–56. Epub 2014/12/24. <https://doi.org/10.1161/CIRCRESAHA.116.305404> PMID: 25532796; PubMed Central PMCID: PMC4344847.
  33. Chou AC, Ju YT, Pan CY. Calmodulin Interacts with the Sodium/Calcium Exchanger NCX1 to Regulate Activity. *PloS one*. 2015; 10(9):e0138856. <https://doi.org/10.1371/journal.pone.0138856> PMID: 26421717; PubMed Central PMCID: PMC4589332.
  34. Weber CR, Ginsburg KS, Philipson KD, Shannon TR, Bers DM. Allosteric regulation of Na/Ca exchange current by cytosolic Ca in intact cardiac myocytes. *J Gen Physiol*. 2001; 117(2):119–31. <https://doi.org/10.1085/jgp.117.2.119> PMID: 11158165; PubMed Central PMCID: PMC2217247.
  35. Machado FS, Tanowitz HB, Ribeiro AL. Pathogenesis of chagas cardiomyopathy: role of inflammation and oxidative stress. *Journal of the American Heart Association*. 2013; 2(5):e000539. Epub 2013/10/25. <https://doi.org/10.1161/JAHA.113.000539> PMID: 24152984; PubMed Central PMCID: PMC3835267.
  36. Bonney KM, Engman DM. Chagas heart disease pathogenesis: one mechanism or many? *Current molecular medicine*. 2008; 8(6):510–8. Epub 2008/09/11. <https://doi.org/10.2174/156652408785748004> PMID: 18781958; PubMed Central PMCID: PMC2859714.
  37. Higuchi Mde L, Benvenuti LA, Martins Reis M, Metzger M. Pathophysiology of the heart in Chagas' disease: current status and new developments. *Cardiovascular research*. 2003; 60(1):96–107. Epub 2003/10/03. [https://doi.org/10.1016/s0008-6363\(03\)00361-4](https://doi.org/10.1016/s0008-6363(03)00361-4) PMID: 14522411.